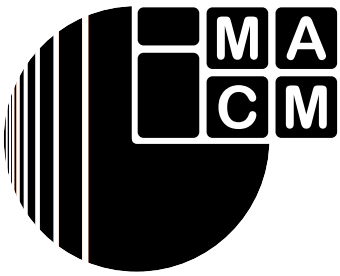

Bergische Universität Wuppertal

Fachbereich Mathematik und Naturwissenschaften

Institute of Mathematical Modelling, Analysis and Computational Mathematics (IMACM)

Preprint BUW-IMACM 11/13

Sebastian Schöps, Herbert De Gersem and Andreas Bartel

Higher-Order Cosimulation of Field/Circuit Coupled Problems

July 2011

http://www.math.uni-wuppertal.de

Higher-Order Cosimulation of Field/Circuit Coupled Problems

Sebastian Schöps[1], Herbert De Gersem[2], and Andreas Bartel[1]

[1] Bergische Universität Wuppertal, Gaußstraße 20, 42119 Wuppertal, Germany
[2] Katholieke Universiteit Leuven, Etienne Sabbelaan 53, 8500 Kortrijk, Belgium

This paper discusses the weak coupling of nonlinear magnetoquasistatic field models (e.g. of induction motors) to an external electric network model (e.g. of frequency converters). A piece-wise linear inductance (as lumped field model) is not sufficiently accurate if the magnetic field exhibits strong eddy current effects. Here, we propose to represent the field model in the circuit equations by a more complex surrogate model. It is fitted by dynamic iteration ('waveform relaxation') during the cosimulation procedure. We demonstrate the link between dynamic iterations and the achievable convergence order of the time integrator numerically.

***Index Terms*—Coupling circuits, Eddy currents, Iterative algorithms, Differential-equations, Convergence of numerical methods.**

I. Introduction

FOR field-circuit coupled models of electrical energy transducers, two general approaches are well established. A first approach consists of extracting lumped parameters or surrogate models from a field model and inserting these as a netlist into a Spice-like circuit simulator. Then, time dependent phenomena (e.g. saturation, eddy currents, hysteresis) require quite elaborated surrogate modeling. This is circumvented by the second approach, monolithic coupling, where field and circuit model are solved together. This, however, necessitates specialized time integration and solving techniques.

We propose a particular synthesis, [1]. Based on commonly defined *time windows* and intermediate *synchronization points*, the electric circuit model and the magnetic field model are solved independently with a possibly different time step from one to the next synchronization point. Intermediate solutions and on-the-fly calculated lumped parameters are exchanged at the synchronization points. A *dynamic iteration*, i.e., repeating the time window with updated information, guarantees a tight coupling between the subproblems. This approach is a true two-way coupling and naturally enables different time steps and solution techniques for each subsystem.

In this paper, we show that adapting the surrogate model and repeating the time window is necessary to realize a higher order convergence of the overall time integration, in particular when nonlinearities and motional effects are included. A classical operator splitting approach (e.g. Yanenko splitting) without iterations only achieves a first order splitting error, [2]. We will show that a higher order time integration of the subproblems makes only sense when carrying out an accordingly chosen number of dynamic iterations.

II. Benchmark Model: Oscillator

Let us consider a simple oscillator circuit, see Fig. 1. For simplicity we describe here the circuit in minimal coordinates, i.e., in the electric voltages u at the nodes 1 and 2:

$$\dot{u}_1 = \frac{R}{L(i)}(u_2 - u_1), \quad \dot{u}_2 = \frac{1}{RC}\left(V_{\text{op}} - u_1\right) - \frac{1}{C}g(u_2). \quad (1)$$

The inductance L is described by a nonlinear magnetostatic

Manuscript submitted to IEEE. Corresponding author: Sebastian Schöps (e-mail: schoeps@math.uni-wuppertal.de)

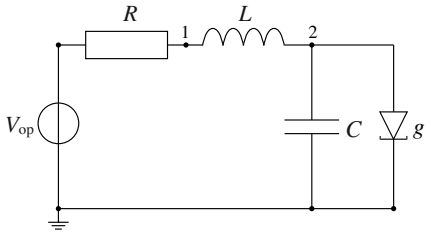

Fig. 1. Tunnel diode oscillator with parameters $C = 0.05$F, $R = 0.5\Omega$, $V_{\text{op}} = 0.25$V and diode $g(v) = -v$, s.t. explicit time integration is feasible.

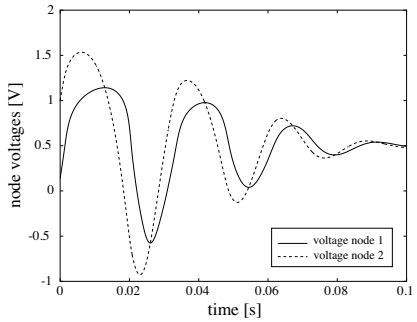

Fig. 2. Nodal voltages of the oscillator circuit shown in Fig. 1.

partial differential equation (PDE) model, the curlcurl equation. Spatially discretized (e.g. by FEM, [3]), it reads:

$$\mathbf{K}(\mathbf{a})\mathbf{a} - \mathbf{X}i = 0, \quad (2)$$

where $\mathbf{a}$ is the line-integrated magnetic vector potential, $\mathbf{K}$ is the nonlinear curl-curl-reluctance matrix and $\mathbf{X}$ is the winding function that describes the current distribution in the coil. This inductor model is excited by the current $i = (V_{\text{op}} - u_1)/R$. The waveforms for the node voltages are given in Fig. 2.

Solving (2) partially for $\mathbf{a}$, we can extract the inductance

$$L(\mathbf{a}) := \mathbf{X}^\top \left(\mathbf{K}(\mathbf{a})\right)^{-1} \mathbf{X}$$

for insertion in (1). Doing so, we defined a two-way coupled system which will be explored in the next section.

III. Cosimulation

The coupled system (1-2) reads in semi-explicit form as:

$$\dot{\mathbf{u}} = \mathbf{f}(\mathbf{u}, L) \quad \text{and} \quad 0 = \mathbf{g}(\mathbf{u}, L).$$

The cosimulation is organized as a Gauß-Seidel-scheme. The time interval of interest $[0, T]$ is subdivided into a series of

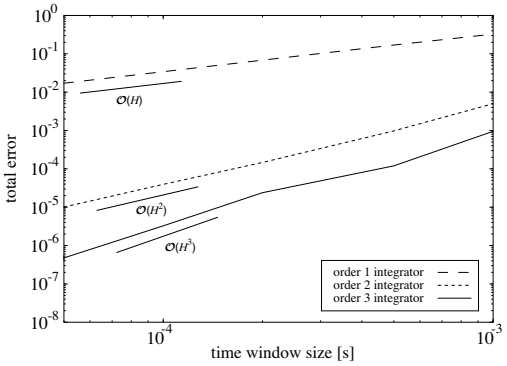

Fig. 3. Convergence plot of cosimulation with $n = 3$ iterations per window using constant extrapolation and cubic interpolation.

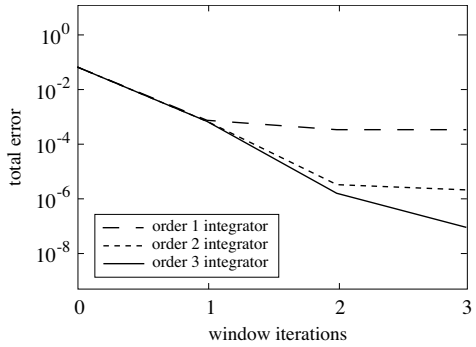

Fig. 4. Contraction of solution on the first time window $[0,\ 5 \cdot 10^{-5}]$s for increasing iterations $k = 1, \ldots, 3$ and methods of different order.

time windows: $0 = T_0 < T_1 < \cdots < T_n = T$ with synchronization points T_i and window sizes $H_i = T_{i+1} - T_i$. The circuit and field problems are sequentially solved on those windows $[T_i, T_{i+1}]$. The waveforms are exchanged iteratively on each time window, i.e., the field problem is recomputed on a time window by using the new circuit waveforms etc.

$$\dot{\mathbf{u}}^{(k+1)} = \mathbf{f}(\mathbf{u}^{(k+1)}, L^{(k)}) \quad \text{and} \quad 0 = \mathbf{g}(\mathbf{u}^{(k+1)}, L^{(k+1)}),$$

where the superscript $k = 1, \ldots, m$ denotes the iteration number, see [4] and the special case $m = 1$ in [5], [6].

Notice, the inductance $L = L(t)$ is now considered as a waveform that depends on time instead of currents or magnetic vector potentials. This introduces splitting errors: on each time windows we solve the subsystems separately. The first waveform ($k = 0$) is extrapolated from previous solutions.

IV. Higher Order Cosimulation

In [2], [7] it has been shown that iterations are not only necessary for improving stability but also for fully exploiting the accuracy of higher order time integration of the subproblems. For the given problem the splitting error decreases by $\mathcal{O}(H)$ with each dynamic iteration.

For the benchmark problem (1-2) both subsystems are discretized with the same time step size $h_i = H_i/4$. This test case setting is chosen to demonstrate the error behavior for our cubic spline interpolation described below. Thus the waveforms on $[T_i, T_{i+1}]$ are given as discrete values, e.g. $L^{(k+1)}(t_j)$ with $t_j = T_i + j \cdot H_i/4$ and $j = 0, \ldots, n_i = 4$. We solved the circuit problem by Runge-Kutta methods of orders 1, 2 and 3. The continuous waveforms are recovered from the discrete values by cubic spline interpolation. This is necessary because single step methods compute their higher order approximations by evaluating the right-hand-side function at intermediate time instants and therefore the approximation order of the interpolation should match the order of the time integration. For the cosimulation we applied $m = 3$ dynamic iterations and used various window sizes $H = 5 \cdot 10^{-5}, \ldots, 5 \cdot 10^{-3}$. The results are compared to a monolithic reference solution of high accuracy. As expected, the convergence order of the time integration error is $\mathcal{O}(H^p)$ where p is the order of the subproblem time integrators (Fig. 3).

Due to the sequential computation of solutions for the subsystems, we introduce a splitting error. This error is controlled by the number of dynamic iterations. Fig. 4 shows the reduction of the splitting error on a single window due to additional iterations. The first order time integration does not benefit from the additional iterations 2 and 3 because the time discretization error dominates here (the analog argument holds true for the second order approximation). Hence to preserve the overall order, three iterations are only mandatory in combination with third order subproblem time integrators. Furthermore less iterations will destroy the global convergence property, Fig. 5. To achieve a prescribed temporal convergence order, one needs to conscientiously select both the subproblem time integration methods, the interpolation and the number of dynamic iterations. Approaches without iteration, e.g., [5], [6], should only be used in combination with first order integrators.

In practice the problem is more involved because each subproblem may be described by a dynamical system (e.g. the field part is magnetoquasistatic). Furthermore the problems are not formulated in minimal coordinates (e.g. the circuit might me modeled by modified nodal analysis) and then the cosimulation might diverge, see [8]. Then window iterations are even more important to guarantee stability and higher order accuracy. In the end one will use different time steps for the field and circuit subproblems to exploit multirate, [4].

V. Electrical Machines and Multirate

Let us discuss the cosimulation of more complicated devices, e.g. the induction machine depicted in Fig. 6. This example necessitates to consider eddy currents, saturation and rotor movement. Since these effects typically occur at different time scales, we have *multirate* behavior. The magnetoquasistatic model with circuit-coupling reads

$$\mathbf{M}\frac{\mathrm{d}}{\mathrm{d}t}\mathbf{a} + \mathbf{K}(\mathbf{a},\theta)\mathbf{a} - \mathbf{X}\mathbf{i} = 0, \quad \mathbf{X}^\top \frac{\mathrm{d}}{\mathrm{d}t}\mathbf{a} + \mathbf{R}\mathbf{i} = \mathbf{v}. \quad (3)$$

As above, $\mathbf{a}$ denotes the line-integrated magnetic vector potential. $\mathbf{R}$, $\mathbf{i}$ and $\mathbf{v}$ are the DC resistance matrix, currents and voltage drops of the coils. Each column of the matrix $\mathbf{X}$ is a discretization of a winding function. $\mathbf{M}$ is the conductivity matrix and $\mathbf{K}$ is the curl-curl-reluctivity matrix. For an electrical machine, $\mathbf{K}$ additionally depends on the rotor angle θ (Fig. 6). This angle solves the motion equation

$$m\frac{\mathrm{d}^2}{\mathrm{d}t^2}\theta + \lambda\frac{\mathrm{d}}{\mathrm{d}t}\theta = f(\mathbf{a}) \quad (4)$$

with mass moment of inertia m, friction coefficient λ and force f.

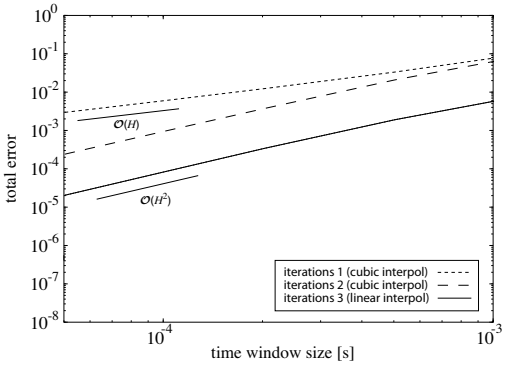

Fig. 5. Convergence plot of cosimulation with 3rd order integrator using constant extrapolation (higher order accuracy is lost for $m < 3$).

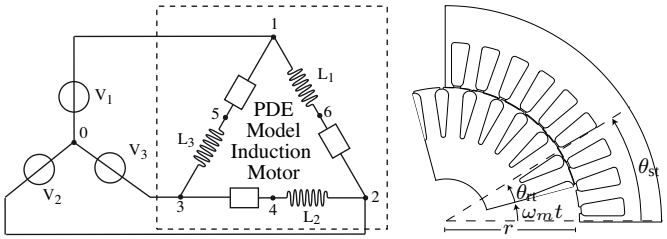

(a) Circuit with pulsed voltage sources. (b) Angle and angular speed.

Fig. 6. Induction machine: circuit and induction machine.

A. Circuit Coupling by the Schur Complement

The PDE (3) can be solved (partially) for $\mathbf{a}$

$$\mathbf{a} = \mathbf{K}^{-1}(\mathbf{a},\theta)\mathbf{X}\mathbf{i} - \mathbf{K}^{-1}(\mathbf{a},\theta)\mathbf{M}\frac{\mathrm{d}}{\mathrm{d}t}\mathbf{a},$$

and then inserted into the coupling equation (3):

$$\frac{\mathrm{d}}{\mathrm{d}t}\Big(\underbrace{\mathbf{X}^\top\mathbf{K}^{-1}(\mathbf{a},\theta)\mathbf{X}}_{:=\mathbf{L}(\mathbf{a},\theta)}\mathbf{i} - \underbrace{\mathbf{X}^\top\mathbf{K}^{-1}(\mathbf{a},\theta)\mathbf{M}\frac{\mathrm{d}}{\mathrm{d}t}\mathbf{a}}_{:=\mathbf{\Phi}_{\mathrm{eddy}}(\mathbf{a},\theta)}\Big) + \mathbf{R}\mathbf{i} = \mathbf{v}. \quad (5)$$

This generalizes the Schur complement inductance extraction. If the lumped equations (5) are updated at every time point according to (3), then they exactly describe all effects of the field part needed within the circuit. This evaluation comes with additional cost and is not recommended within a strong coupling. For a weak coupling as proposed here, this observation motivates a multirate time stepping technique.

B. Cosimulation Essentials

We simulate the circuit and field subproblems independently from each other on time windows using the cosimulation approach as described in Section III. The algorithm is applied to the field-circuit coupled induction machine model. The circuit subproblem is solved with given waveforms for $\mathbf{v}(t)$ and $\theta(t)$ and delivers solutions for $\mathbf{L}(t)$, $\Phi_{\text{eddy}}(t)$ and $f(t)$. $\mathbf{L}(t)$ and $\Phi_{\text{eddy}}(t)$ serve as inputs for the circuit model, whereas $f(t)$ serves as input for the equation of motion. It is important to recognize that the dependencies of $\mathbf{L}$ and $\mathbf{\Phi}_{\text{eddy}}$ (e.g. the angle θ) become a dependence on time t, because of the waveform relaxation approach, i.e., they are assumed to be known functions for the circuit problem. The computation of field and circuit are successively solved in a dynamic iteration in order to preserve the convergence order of the subproblem time integrators at the time window level and in order to guarantee the stability of the overall time integration process.

C. Multirate Dynamics of Nonlinear Effects

Often the physical relevant time scales are not well separated in the coupling variables. We imagine an induction motor driven by a pulse-width-modulated voltage source, which is switching at 20kHz and carries a 50Hz signal, cf. [4]. The circuit variables must be sampled on the fast scale, but the dynamics of the extracted inductance matrix is governed by the smaller frequency. Here the magnetic saturation of a nonlinear material (PDE model) depends on the supplied energy, which is related to the time integral of the applied voltage $\mathbf{v}(t)$

$$\psi(t) = \textstyle\int_0^t \mathbf{v}(s)\mathrm{d}s.$$

The relevant nonlinear behavior is described on the time scale of this integral even if the applied voltage is a much faster signal. In our example [4], the integral is a step function (sampled at 20kHz), which approximates a cosine of 50Hz. From another point of view, quantities are often composites

$$\mathbf{v}(t) = \mathbf{v}_{\text{fast}}(t) + \mathbf{v}_{\text{slow}}(t),$$

of a fast $\mathbf{v}_{\text{fast}}$ and a slow part $\mathbf{v}_{\text{slow}}$ and the governing time rate is given by $\mathbf{v}_{\text{slow}}$; typically either the amplitude of the fast signal $\max|\psi_{\text{fast}}| \ll \max|\psi_{\text{slow}}|$ is negligible or the energy of the fast switching signal $\mathbf{v}_{\text{fast}}(t)$ is evolving at a slower time rate. In either case, the impact of the fast signal on the nonlinear effects can often be disregarded. This is also valid in thermal coupling [9], which is effective on a slower time scale due to energy transport. Thus the field model fed by the underlying slow signal will have the same effect as the fast waveform, but the time integration will need fewer time steps.

Since the underlying, driving waveforms (as $\mathbf{v}_{\text{slow}}$) are typically not given or might by modified by additional circuit elements, we need a method to uncover these signals. Among various possibilities, we propose here a simple method based on spline interpolation of the integrated voltage.

The known waveform $\mathbf{v}(t)$ is integrated on $\mathcal{I} = [T_i,\ T_{i+1}]$. This corresponds to the discrete summation of $\mathbf{v}(t_j)$ ($t_j \in \mathcal{I}$) weighted by with time step h_j: (rectangle rule)

$$\psi_l := \sum\nolimits_{j=1}^{l} \mathbf{v}(t_j)h_j \qquad (l = 0,\ldots,n_i). \quad (6)$$

Now we define a cubic spline interpolation $\tilde{\psi}(t)$ of $(t_{l^*},\ \psi_{l^*})$. This gives a smooth time-integrated voltage. The interpolation knots t_{l^*} should be chosen according to the dynamics of the underlying (slow) waveform. E.g. the number of knots can easily be estimated by a Fourier analysis or might by known beforehand. It is crucial that the spline is a good approximation of (6), because otherwise the energy balance will be violated.

Finally, the cubic spline interpolation is differentiated with respect to time. This yields a slowly varying spline approximation $\tilde{\mathbf{v}}_{\text{slow}}(t)$ of the underlying waveform. Obviously, the smooth signal requires a smaller number of time steps for representation than the original fast switching signal.

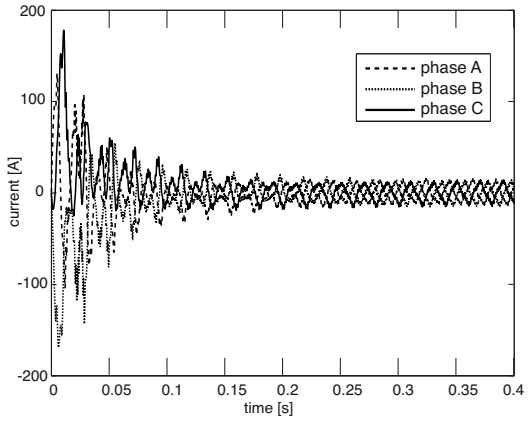

Fig. 7. Currents through induction machine during start-up

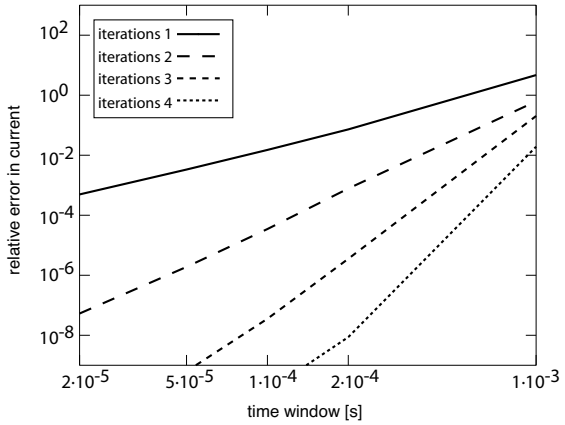

Fig. 8. Convergence of higher order cosimulation for the problem from [4].

D. Simulation of Motor and Transformer

The proposed scheme was implemented in `FIDES` and `OCS` from the CoMSON project, for the meshing `Triangle` embedded in `FEMM` was used, [10], [11]. Our implementation supports nonlinear materials, eddy currents and motion. Various time integrators are available. We report on two examples.

For the induction machine Fig. 6, the explicit Euler method was used for the equation of motion and the implicit Euler method for the field and circuit equations. The field and motion equations are integrated with time steps of 10^{-5}s, 10^{-4}s or $5 \cdot 10^{-4}$s. The circuit including the lumped field model used 10^{-6}s. The obtained currents are given in Fig. 7. Hence the number of time steps for the field problem were reduced from 400000 for a strong coupled monolithic approach to 800 for the cosimulation scheme. The nonlinear behavior of the motor in the inrush current phase was computed by both a strong and weak cosimulation approach. In the strong coupled simulation, field and circuit equations were discretized by time steps of 10^{-6}s. The cosimulation uses constant window sizes that match the step sizes of the field problem, i.e., $H = 10^{-5}$s, 10^{-4}s and $5 \cdot 10^{-4}$s. One dynamic iteration ($m = 1$) is sufficient for this particular configuration because of the simple surrounding circuit and more generally because of the first order time integration.

The maximal relative errors occur at the time instant of maximal current, where a very high level of saturation is reached. For the time step size $5 \cdot 10^{-4}$s the error is ca. 10%, while for step sizes 10^{-5}s and 10^{-4}s the error is less than 5%. This is close to the expected time discretization error for a signal switching at 20kHz. Furthermore the accuracy is in the range of the typical measurement error for the nonlinear material curve. A higher accuracy can always by achieved by using smaller time steps or in the case of more complicated circuits by additional iterations.

To demonstrate this, our second example is a transformer in a lowpass-filter circuit, [4]. It was solved by a 5th order implicit Runge-Kutta scheme (RADAU5) for different iteration numbers ($k = 1, \ldots, 4$). The error behavior is given in Fig. 8. In this particular example the gain per iteration is $\mathcal{O}(H^2)$.

The computational efforts of the cosimulations are significantly smaller than in the strong coupling: less time steps yield less computational time, e.g. the cosimulation of the induction machine takes a couple of minutes while the computation of the standard single-rate solution requires about 12h on a desktop PC (which serves here as reference solution).

VI. Conclusions

Cosimulation was proven to be a flexible approach enabling different time steps for each subproblem (multirate). To achieve a respective convergence order we demonstrated that the number of iterations had to be carefully chosen. For field/circuit problems the time rate of the saturation is driven by the delivered energy. This rendered the field in our application as slower subsystem. For a fast cosimulation, we defined a coupling extracting the slower time scale by signal separation, i.e., the nonlinear field part for the lumped model is updated with an accordingly slower sample rate. A substantial reduction of computation time has been achieved.

References

[1] G. Bedrosian, "A new method for coupling finite element field solutions with external circuits and kinematics," *IEEE Trans Magn*, vol. 29, no. 2, pp. 1664 – 1668, 1993.

[2] P. K. Vijalapura, J. Strain, and S. Govindjee, "Fractional step methods for index-1 differential algebraic equations," *J Comput Phys*, vol. 203, no. 1, pp. 305 – 320, 2005.

[3] N. Sadowski, B. Carly, Y. Lefevre, M. Lajoie-Mazenc, and S. Astier, "Finite element simulation of electrical motors fed by current inverters," *IEEE Trans Magn*, vol. 29, no. 2, pp. 1683–1688, Mar. 1993.

[4] S. Schöps, H. De Gersem, and A. Bartel, "A cosimulation framework for multirate time-integration of field/circuit coupled problems," *IEEE Trans Magn*, vol. 46, no. 8, pp. 3233 – 3236, 2010.

[5] P. Zhou, D. Lin, W. N. Fu, B. Ionescu, and Z. J. Cendes, "A general co-simulation approach for coupled field-circuit problems," *IEEE Trans Magn*, vol. 42, no. 4, pp. 1051 – 1054, Apr. 2006.

[6] E. Lange, F. Henrotte, and K. Hameyer, "An efficient field-circuit coupling based on a temporary linearization of FE electrical machine models," *IEEE Trans Magn*, vol. 45, no. 3, pp. 1258–1261, 2009.

[7] A. Bartel, M. Brunk, M. Günther, and S. Schöps, "Dynamic iteration schemes for coupled problems in circuit/device simulation," 2011, in prep.

[8] M. Arnold and M. Günther, "Preconditioned dynamic iteration for coupled differential-algebraic systems," *BIT*, vol. 41, no. 1, pp. 1 – 25, 2001.

[9] J. Driesen, R. J. M. Belmans, and K. Hameyer, "Methodologies for coupled transient electromagnetic-thermal finite-element modeling of electrical energy transducers," *IEEE Trans Ind Appl*, vol. 38, no. 5, pp. 1244–1250, Sep. 2002.

[10] J. R. Shewchuk, "Triangle: Engineering a 2D Quality Mesh Generator and Delaunay Triangulator," *Applied Computational Geometry: Towards Geometric Engineering*, pp. 203–222, 1996.

[11] D. Meeker, *FEMM User's Manual*, 2010, version 4.2 (09Nov2010 Build). [Online]. Available: http://www.femm.info/